
Deep learning improved by biological activation functions

Gardave S. Bhumbra*

Department of Neuroscience, Physiology and Pharmacology,
UCL, Gower St.,
London (UK), WC1E 6BT.
g.bhumbra@ucl.ac.uk

Abstract

‘Biologically inspired’ activation functions, such as the logistic sigmoid, have been instrumental in the historical advancement of machine learning. However in the field of deep learning, they have been largely displaced by rectified linear units (ReLU) or similar functions, such as its exponential linear unit (ELU) variant, to mitigate the effects of vanishing gradients associated with error back-propagation. The logistic sigmoid however does not represent the true input-output relation in neuronal cells under physiological conditions. Here, bionodal root unit (BRU) activation functions are introduced, exhibiting input-output non-linearities that are substantially more biologically plausible since their functional form is based on known biophysical properties of neuronal cells.

In order to evaluate the learning performance of BRU activations, deep networks are constructed with identical architectures except differing in their transfer functions (ReLU, ELU, and BRU). Multilayer perceptrons, stacked auto-encoders, and convolutional networks are used to test supervised and unsupervised learning based on the MNIST and CIFAR-10/100 datasets. Comparisons of learning performance, quantified using loss and error measurements, demonstrate that bionodal networks both train faster than their ReLU and ELU counterparts and result in the best generalised models even in the absence of formal regularisation. These results therefore suggest that revisiting the detailed properties of biological neurones and their circuitry might prove invaluable in the field of deep learning for the future.

1 Introduction

Neurobiology has inspired the design of computational networks ever since they were first conceived (Hassabis et al., 2017). When the ‘perceptron’ classifier was introduced (Rosenblatt, 1958), the non-linearity used to characterise the input-output relationship was based on a critical input boundary above which outputs were fully activated, resembling the ‘threshold’ and ‘all-or-none’ properties of neurones (Hodgkin and Huxley, 1952). Continuous ‘activation’ or ‘transfer’ functions, such as the sigmoid non-linearity (Figure 1), were employed subsequently to represent the output of units as analogous to neuronal firing rates (Dayan and Abbott, 2001).

With the advance of deep learning however ‘biologically-inspired’ activation functions have been largely supplanted by non-linearities that possess a linear component in the positive polarity (Nair and Hinton, 2010; Glorot et al., 2011). A key advantage of these more recent transfer functions, notably the rectified linear unit (ReLU, Figure 1), is that their non-contractive positive activations mitigate the effects of vanishing gradients associated with error back-propagation. Since

*Website: www.deepnodal.net

the deep learning performance of the ReLU activation function and its variants usually exceed that of their sigmoid predecessors that confer no such advantage, the utility of ‘biological insights’ into input-output relationships might be called into question.

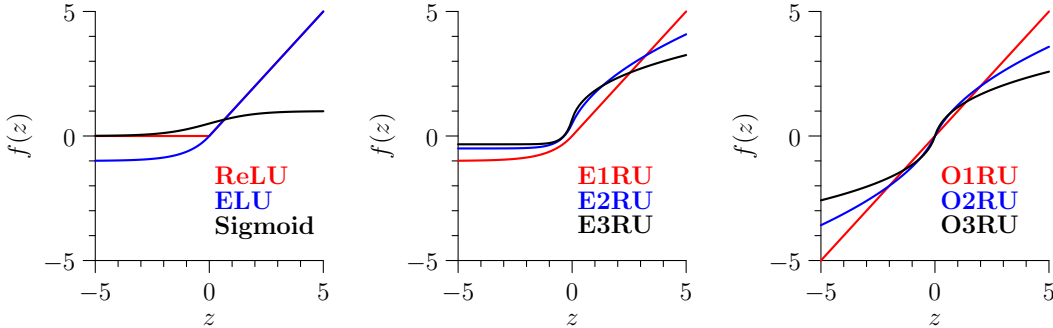


Figure 1: Graphs of activation functions. The left overlays the standard logistic sigmoid function, rectified linear unit (ReLU), and exponential linear unit (ELU). Bionodal root unit (BRU) transfer functions are shown for exponential root units (ERU, middle) and odd root units (ORU, right), for radices: $r = \{1, 2, 3\}$.

Electrophysiological recordings (Binder et al., 2011) and biophysical simulations (Fourcaud-Trocmé et al., 2003; Bhumbra et al., 2014) of neurones however show that their input-output relationships are not sigmoid. At rheobase, which defines the minimum positive current required to evoke a single output discharge, only modest increments in depolarising inputs are required to accelerate firing in many neuronal types. This acceleration results from active conductances, mediated by voltage-sensitive ion channels, that overcome passive leak conductances and drive neuronal firing of action potentials. However, after an initial linear slope in the input-output relation, the response curve only partially saturates as the voltage-sensitive channels become increasingly inactivated.

It is possible to induce depolarisation experimentally to the extent of inactivating voltage-sensitive channels completely. While this observation is consistent with the theoretical concept of a maximum output discharge rate, the size of the necessary depolarisation is well beyond the physiological range. Therefore the suggestion that the input-output relationship in biological neurones fully saturates represents as little useful scientific insight as the suggestion that the ReLU activation must saturate in practice due to the finite numeric range of computer floating point units.

Here, a family of transfer functions termed bionodal root units (BRU), are introduced which are substantially more biologically plausible than sigmoid activations. BRU activation functions were devised on basis of the biophysical properties of neuronal cells rather than as a result of theoretical optimisations of deep learning models. The present study compares the deep learning performance of bionodal networks to that of identical networks that differ only in their activation using either the ReLU transfer function or one of its variants (Clevert et al., 2015) called the ‘exponential linear unit’ (ELU, Figure 1).

2 Methods

2.1 Bionodal root units

BRU activations comprise two subfamilies, namely the exponential root units (ERU) and odd root units (ORU) which can be combined for different layers within a deep network. The exponential root unit (ERU) is:

$$f(z) = \begin{cases} (r^2 z + 1)^{\frac{1}{r}} - \frac{1}{r}, & \text{if } z \geq 0 \\ e^{rz} - \frac{1}{r}, & \text{if } z < 0 \end{cases}, \quad \frac{df(z)}{dz} = \begin{cases} r(r^2 z + 1)^{\frac{1-r}{r}}, & \text{if } z \geq 0 \\ r e^{rz}, & \text{if } z < 0 \end{cases} \quad (1)$$

where the radix r is a positive shape parameter that defines the choice of non-linearity. The ERU is monotonic and its derivative is continuous everywhere including at $z = 0$, where the derivative is at its maximum r . A root function was chosen on the basis of the successful use of square root functions to fit current-frequency relationships observed in current-clamp recordings from neurones (Ermentrout, 1998) and those obtained from biophysical models (Fourcaud-Trocmé et al., 2003). Adoption of a square root function is analogous to an ERU with a radix r of 2, which is termed the exponential 2nd root unit (E2RU, Figure 1). The first root (E1RU, Figure 1) is equivalent to the ELU transfer function. For higher root units, the derivative is decreasing in the positive polarity but does not asymptote to zero, unlike in the negative polarity. At the limit where $r \rightarrow \infty$, the ERU tends to a Heaviside step function.

The odd radical root unit (ORU) is:

$$f(z) = \text{sgn}(z)((r^2|z| + 1)^{\frac{1}{r}} - 1) \quad , \quad \frac{df(z)}{dz} = r(r^2|z| + 1)^{\frac{1-r}{r}} \quad (2)$$

where once again the radix r is a positive shape parameter that defines the choice of non-linearity. Like the ERU, the ORU is monotonic and its derivative is continuous everywhere including at $z = 0$, where the derivative is at its maximum r . However unlike the ERU, the symmetrical functional form of the ORU makes the activation function odd. The first root (O1RU, Figure 1) corresponds to the identity function. For higher root units, the magnitude of the derivative decreases in both polarities but does not asymptote to zero. Therefore while the profile of ORU functions may resemble the hyperbolic tangent, ORU activations are not asymptotically bounded.

Methods of initialising weight coefficients based on scaling second moments (Glorot and Bengio, 2010) aim to regulate variances of activations propagated throughout hidden layers. Recent optimisation of this technique for ReLU networks (He et al., 2015) adopts a Gaussian initialisation with variances scaled by $2/n_i$, where n_i is the number of inputs. While such scaling would be suitable for BRU transfer functions with a radix r of 1, it is not optimal for the greater curvatures exhibited by higher radices. The variance σ^2 scaling adopted for BRU layers was therefore assigned empirically using reciprocal relations with the radix r :

$$\sigma^2(\text{ERU}) = \frac{6}{n_i(2r + 1)} \quad (3)$$

$$\sigma^2(\text{ORU}) = \frac{2}{n_i r} \quad (4)$$

When r is 1, this would result in a scaling for E1RU and O1RU weight initialisation that would be identical to the standard fan-in method (He et al., 2015). Output layers employing softmax or sigmoid functions were initialised using identical variance scaling. During experiments, ReLU and ELU network weight coefficients were also initialised in the same way. In all layers with weight coefficients, bias offset parameters were trainable and initialised to $\mathbf{b} = \mathbf{0}$. No attempt was made to tune learning rates, which were set to a constant value at an order of magnitude that resulted in no initial divergent learning in networks for any the three transfer functions. Experiments were run for 200 epochs, and conducted using the TensorFlow machine learning framework (Abadi et al., 2015).

3 Results

3.1 Multilayer perceptron supervised learning

Since the two subfamilies of activations functions as well as the corresponding weight initialisation procedures presented in this study are novel, simple experiments were first conducted to confirm that BRU non-linearities facilitate learning in networks of increasing depth. Fully connected multilayer perceptron networks, with the number of hidden layers ranging from 4 to 8, were trained on the MNIST data set (60000 training and 10000 test samples of 28x28 images). In order to allow comparisons with previous work (Clevert et al., 2015), the architectures and training parameters were matched with 128 units in each hidden layer, a learning rate η of 0.01, a batch size of 64, a softmax output activation, a cross entropy loss function, and a stochastic gradient descent learning update. In

correspondence with the MNIST dataset dimensionality, the input data dimension was 784, and the number of output units was 10.

Transfer functions for hidden layers were either ReLU, ELU, or BRU functions. BRU subtypes were assigned according to the following scheme: O3RU for the first hidden layer, E2RU for the last hidden layer, and O2RU for intervening hidden layers. This permutation was selected to facilitate back-propagation of gradients, to center activations within the inner hidden layers close to zero, and to produce a sparse encoding input to the softmax output layer. Initial training and test loss values are plotted for each the three types of networks in Figure 2.

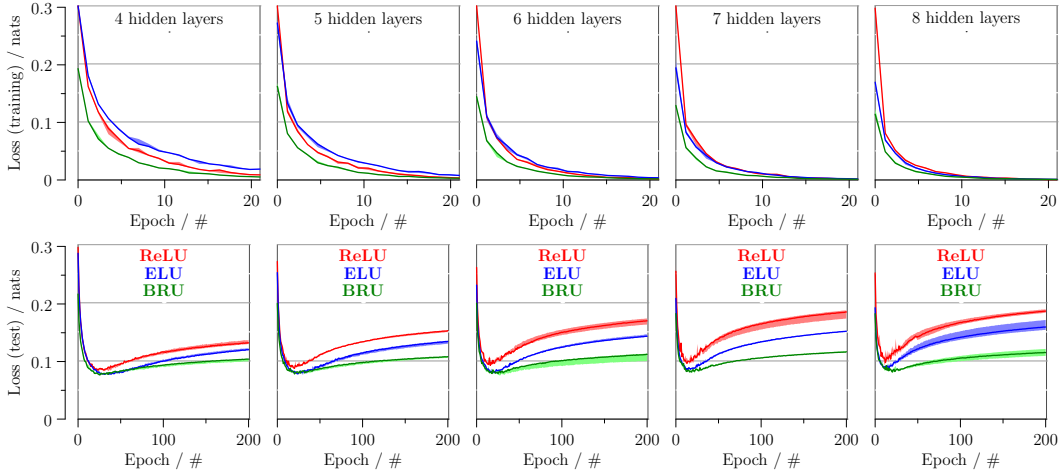


Figure 2: Multilayer perceptron training on the MNIST data set with 4 to 8 hidden layers. Networks employing ReLU, ELU, and BRU activation functions were trained, and the loss for training and test sets from several runs are plotted as lines for the medians and bands for the inter-quartile ranges.

Training cross entropy losses plotted in the top row of Figure 2 show that with 4 hidden layers, the ELU network is the slowest in training. While the ReLU network is somewhat faster, the bionodal network is the fastest. With 6 hidden layers, the training performance of the ReLU and ELU networks have both improved with similar training loss profiles but the RRU network remains faster. For the 8 hidden layer network, which repeats precisely the experiment of Clevert et al. (2015), the ELU network outperforms the ReLU network, confirming the findings of the previous study. The bionodal network however still maintains its lead in performance as the fastest learning network of the three.

Test cross entropy losses plotted in the bottom row of Figure 2 show that with 4 hidden layers, ELU networks generalise better ReLU networks. While the bionodal network shows the fastest reduction in test loss, it is also relatively refractory to test loss increases compared to the other networks at the overfitting stage. As the number of hidden layers is increased, the ReLU and ELU networks increasingly overfit with the ReLU networks being the more sensitive. By contrast, overfitting in the bionodal networks is less affected by changes in the number of hidden layers, and results in the lowest minimum test loss of the three networks during training with 8 hidden layers. This suggests that the intrinsic capability of bionodal networks to learn generalised models is resistant to the adverse effects of overfitting resulting from increases in depth within the network even in the absence of explicit regularisation.

3.2 Stacked auto-encoder unsupervised learning

Having established BRU transfer functions facilitate supervised learning in networks of increasing depth, a similar experiment was performed to assess unsupervised learning using a stacked auto-encoder network. A standard auto-encoder network design (Hinton and Salakhutdinov, 2006; Desjardins et al., 2015; Clevert et al., 2015) was implemented using a symmetrical architecture with [1000, 500, 250, 30, 250, 500, 1000] units that include both encoder and decoder components with 784 inputs and 784 output units for the MNIST image data. Training parameters

were kept constant using a batch size of 120, a sigmoid transfer function for the output layer, a cross entropy loss function, an Adam (Kingma and Ba, 2014) learning update ($\eta = 0.0001$, $\beta_1 = 0.9$, $\beta_2 = 0.999$, $\epsilon = 0.001$), and weights for the encoder and decoder components were untied.

Transfer functions for hidden layers were either ReLU, ELU, or BRU functions. For BRU networks, the O2RU transfer function was used for all hidden layers apart for the last which was assigned an E1RU function prior to the output layer. In Figure 3, the loss and reconstruction errors are plotted for each the three types of networks for the training test data. The results confirm the findings of Clevert et al. (2015), who show that ELU networks show improved performance over ReLU networks for this auto-encoder architecture. However, bionodal networks outperform both ELU and ReLU networks in all measures of performance.

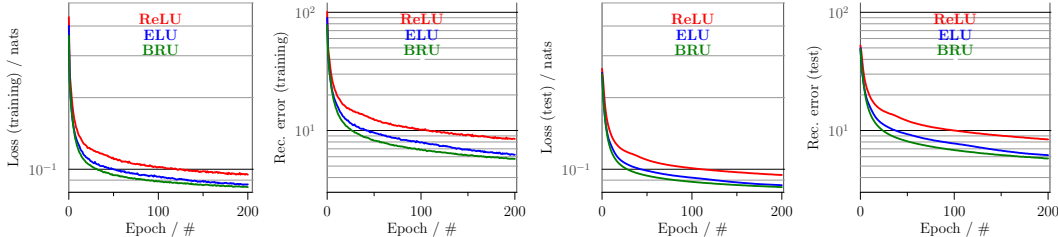


Figure 3: Stack auto-encoder training on MNIST data. Networks employing ReLU, ELU, and BRU activation functions were trained, and the loss and reconstruction errors for training and test sets from several runs are plotted as lines that represent medians.

3.3 Convolutional networks with MNIST data

Since convolutional networks are well adapted for image recognition, they constitute architectures that are suited for the MNIST data set. A convolutional network with a simple architecture was employed to moderate computational complexity for fair and efficient comparison in performance between the activation functions. The architecture was based on the LeNet-5 network (LeCun et al., 1998a): [6 feature maps, 5x5 convolution kernel size, 1 stride], [6 maps, 2x2 average-pool, 2 stride], [16 maps, 5x5 convolution, 1 stride], [16 maps, 2x2 average-pool, 2 stride], [120 maps, 5x5 convolution, 1 stride], 84 fully-connected.

The convolutional network was simplified from the LeNet design in three respects. First, ‘same’ padding was used throughout all convolution and pooling layers. Second, while average pooling layers were used, they did not include learnable parameters and were assigned activation non-linearities for all networks. Finally, output activations were softmax functions with losses calculated using cross entropies. Training and optimisation parameters were identical to those used for the stack auto-encoder experiments described above. Images were zero-centered and rescaled to unit variance. BRU transfer function assignments were as follows: E1RU for all pooling layers, and [E3RU, O2RU, O2RU, E2RU] for the convolution and hidden fully-connected layers.

In Figure 4, the loss and error quotients are plotted for each of the three types of networks for the training data during the initial stage of learning and for the test data for all epochs. The training results support the findings of Clevert et al. (2015), who show that ELU convolutional networks train faster than ReLU networks. The bionodal network however exhibits the fastest learning. While the ELU network initially trains faster than the ReLU network, the test loss and errors quotients show that learning in the ReLU network results in better generalisation. However, bionodal networks outperform both ELU and ReLU networks as measured by the minimum test loss and minimum test error quotient during training. These results suggest that even in the absence of explicit regularisation, the intrinsic capability of bionodal networks to learn generalised models exceeds that of the other networks.

3.4 Convolutional networks with CIFAR data

Simple network designs in the previous MNIST experiments were employed to moderate computational complexity for fair and efficient comparison in performance between the activation functions.

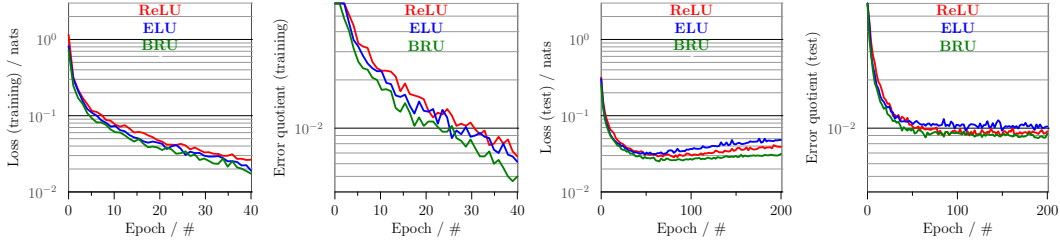


Figure 4: Simplified LeNet convolutional network training on MNIST data.

In order to benchmark more realistic models of deep learning, a more complex network architecture was tested using CIFAR-10/100 data. The CIFAR-10/100 data sets each comprise of 50000 training and 10000 test samples of $32 \times 32 \times 3$ images with 10/100 label classifications.

A 10 hidden-layer network design was based on a ConvPool architecture described previously (Springenberg et al., 2014), with minor modifications to combine same ('S') and valid ('V') padding for different strides: [96, 3x3 convolution, 1S stride], [96, 2x2 convolution, 1V stride], [96, 3x3 max-pool, 2V stride], [192, 3x3 convolution, 1S stride], [192, 3x3 convolution, 1S stride], [192, 3x3 max-pool, 2V stride], [192, 3x3 convolution, 1S stride], [192, 1x1 convolution, 1S stride], [10, 1x1 convolution, 1S stride], [10, 6x6 average pooling, 1S stride], followed by a 10/100 fully-connected softmax output layer. For regularisation, dropout of 50% was applied after each max-pool layer. Images were zero-centered and scaled to unit variance (across all channels), and for each epoch training images were bordered by single zero-value pixels and randomly cropped back to $32 \times 32 \times 3$ sizes then horizontally flipped at random. For bionodal networks, the following BRU transfer functions were assigned to the 10 hidden layers: [E3RU, O3RU, E1RU, E2RU, O2RU, E1RU, E2RU, O2RU, E1RU, E1RU].

In Figure 5, the loss and error quotients are plotted for each the three types of networks for the training data (CIFAR-10 top, CIFAR-100 bottom) during the initial stage of learning and for the test data for all epochs. The CIFAR-10 and CIFAR-100 training results again support the findings of Clevert et al. (2015), who show that ELU convolutional networks train faster than ReLU networks. Consistent with the previous MNIST experiments, the bionodal network exhibits the fastest learning. The results for the CIFAR-10 and CIFAR-100 data sets are notably similar. Both the minimum test loss and test error quotient during training for the ELU networks are lower compared to that of ReLU networks. However, the same measures show that bionodal networks outperform both ELU and ReLU networks. These results confirm that with increases in data dimensionality and architectural complexity, the intrinsic capability of bionodal networks to learn generalised models continues to exceed that of the other networks.

4 Discussion

BRU activation functions were devised on basis of the biophysical properties of neuronal cells. While their derivation was not a result of theoretical optimisations to deep learning models, the results of the present study suggest that bionodal networks train more quickly and generalise better than their ReLU and ELU counterparts. Formal explanation for these behaviours would clearly be merited for future work, but some intuitive deductions that might guide assignment of BRU functions throughout the networks are considered.

4.1 Speed

For all hidden layers the learning speeds during ReLU and ELU training are intrinsically limited homogeneously by the maximum of one in their activation gradients, whereas the maximum gradient for each bionodal layer corresponds to its respective radix r . Differences in the non-linearities across hidden layers in effect lead to different learning speeds throughout the network. Assignment of higher radix BRU transfer functions to initial layers therefore results naturally in faster learning compared to later layers in a manner that can be likened to early layer pre-training. Gradient back-

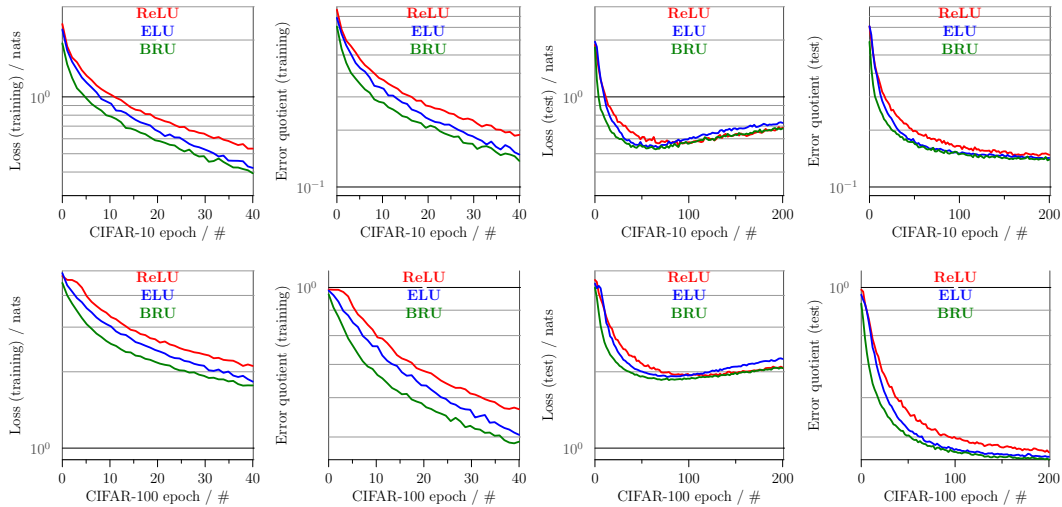


Figure 5: ConvPool network training on CIFAR-10/100 data.

propagation from later layers however is most efficient with lower radix BRU transfer functions that exhibit minimal saturation within their dynamic range.

The non-linearity of transfer functions in early layers is analogous to the response profile of sensory or afferent components of the nervous system. Photoreceptors are one of few mammalian cell subtypes that do not exhibit discrete all-or-none action potentials but graded action potentials. Response curves of photoreceptors to light exhibit considerable non-linearity (Korenbrodt, 2012), conferring cones with the ability to respond to changes in light intensity over several orders of magnitude. This natural phenomenon would suggest assignment of high radix BRU transfer functions to early layers.

Transfer functions towards later layers however would be more analogous to the input-output relation of efferent neuronal components. The final output cell type of the central nervous system is the motoneurone, which transmits all-or-none action potentials to muscles to control movement. Progressive recruitment of motoneurons firing at increasing frequencies induce greater forces of muscle contraction. It is notable that the input-output relation of motoneurons is nearly linear (Heckman et al., 2009), consistent with the assignment of low radix BRU transfer functions to later layers.

4.2 Generalisation

Not only do bionodal networks learn more quickly, but also exhibit an intrinsic capacity to learn models that generalise more effectively compared to ReLU and ELU networks. These findings might challenge the reported sparse encoding advantages attributed to the ReLU transfer function (Glorot et al., 2011). While the linearity in the ReLU and ELU functions may alleviate the effects of vanishing gradients in backpropagation, it may come at the cost of compromising sparsity in the positive activation encoding domain where an unchecked unit gradient risks an underlying tendency to overfit.

It is therefore possible that the solution of mitigating the vanishing gradient using a naïve linearity might be the very cause of how resulting models are impeded in their generalisation without additional regularisation. A scaled exponential linear unit transfer function has been introduced recently (Klambauer et al., 2017) with reported enhancement of regularisation in deep networks through self-normalisation. However this transfer function maintains a linearity in the positive polarity and is therefore likely to be subject to the same impediment.

For radices greater than 1, both ERU and ORU subfamilies would tend towards more sparse encoding models compared to ReLU and ELU transfer functions. Since ERU activations assume a more limited range of negative values, ERU layers would inheritantly result in more sparse encoding than ORU layers of an equivalent radix. Inclusion of ORU transfer functions within hidden layers how-

ever is useful because they bring activations within the inner hidden layers close to zero that results in efficient natural gradient descent Clevert et al. (2015). While the use of symmetrical transfer functions such as the hyperbolic tangent is known to improve deep learning convergence (LeCun et al., 1998b), ORU activations have the advantage of lacking asymptotic limits and therefore obviate the drawbacks of vanishing gradients. The use of ORU functions may also introduce a natural form of self-normalisation with implicit regularisation.

4.3 Future Work

The aim of the present study was to obtain fair comparisons in performance of ReLU, ELU, and BRU transfer functions in deep learning rather than submit a competitive attempt of improving upon current state-of-the-art benchmarks. Optimisations based on weight regularisation, inception multi-convolution learning (Szegedy et al., 2015), batch-normalisation (Ioffe and Szegedy, 2015), and residual learning (He et al., 2016) have been instrumental in recent deep learning advances. However most of these developments have been aimed at improving regularisation within ReLU architectures. While future work would include assessment of how these optimisations could be exploited by bionodal networks, it is likely that some adaption of the techniques will be necessary. For example L1 or L2 regularisation techniques might be somewhat blunt instruments to apply homogeneously to bionodal networks since weight variance initialisation is dependent on the radix which differs across layers.

While experiments have been performed using well established image data sets, it would instructive in future work to extend the scope of research beyond computer vision since transfer functions are universal throughout deep learning networks. For the purposes of simplicity, only very few activation functions from the ERU and ORU subfamilies were used for the present study. It is highly likely that other permutation assignments throughout hidden layers using higher radix non-linearities could improve results dramatically. Since the radix term r is continuous, a potential learning strategy would be to anneal non-linearities during the course of training to optimise sparsity during learning. While empirical approaches were adopted for initialising the weight coefficients, it is probable that implementation of a full theoretical framework underlying parameter initialisation for bionodal layers would further ameliorate learning performance.

The suggestion that the logistic sigmoid function is ‘biological’ would reflect a somewhat incomplete understanding of the excitable properties of neuronal membranes. BRU transfer functions constitute activation non-linearities that are substantially more physiologically plausible. In all experiments of the present study, bionodal networks outperformed their ReLU and ELU counterparts both in terms of speed and generalisation often by considerable margins. It is perhaps true therefore in the understanding of intelligent learning that we should not only look to biology for inspiration, but for solutions.

5 Acknowledgement

The author thanks Maneesh Sahani for helpful discussion and comments on this work.

References

- Abadi M, Agarwal A, Barham P, Brevdo E, Chen Z, Citro C, Corrado GS, Davis A, Dean J, Devin M, Ghemawat S, Goodfellow I, Harp A, Irving G, Isard M, Jia Y, Jozefowicz R, Kaiser L, Kudlur M, Levenberg J, Mané D, Monga R, Moore S, Murray D, Olah C, Schuster M, Shlens J, Steiner B, Sutskever I, Talwar K, Tucker P, Vanhoucke V, Vasudevan V, Viégas F, Vinyals O, Warden P, Wattenberg M, Wicke M, Yu Y, Zheng X (2015) TensorFlow: Large-scale machine learning on heterogeneous systems Software available from tensorflow.org.
- Bhumbra GS, Bannatyne BA, Watanabe M, Todd AJ, Maxwell DJ, Beato M (2014) The recurrent case for the renshaw cell. *J Neurosci* **34**(38):12919–32.
- Binder MD, Heckman C, Powers RK (2011) The physiological control of motoneuron activity. *Comprehensive physiology*.
- Clevert DA, Unterthiner T, Hochreiter S (2015) Fast and accurate deep network learning by exponential linear units (elus). *arXiv preprint arXiv:1511.07289*.

- Dayan P, Abbott LF (2001) *Theoretical neuroscience*, Vol. 806 Cambridge, MA: MIT Press.
- Desjardins G, Simonyan K, Pascanu R et al. (2015) Natural neural networks In *Advances in Neural Information Processing Systems*, pp. 2071–2079.
- Ermentrout B (1998) Linearization of fi curves by adaptation. *Neural computation* **10**(7):1721–1729.
- Fourcaud-Trocmé N, Hansel D, Van Vreeswijk C, Brunel N (2003) How spike generation mechanisms determine the neuronal response to fluctuating inputs. *Journal of Neuroscience* **23**(37):11628–11640.
- Glorot X, Bengio Y (2010) Understanding the difficulty of training deep feedforward neural networks In *Proceedings of the Thirteenth International Conference on Artificial Intelligence and Statistics*, pp. 249–256.
- Glorot X, Bordes A, Bengio Y (2011) Deep sparse rectifier neural networks In *Proceedings of the Fourteenth International Conference on Artificial Intelligence and Statistics*, pp. 315–323.
- Hassabis D, Kumaran D, Summerfield C, Botvinick M (2017) Neuroscience-inspired artificial intelligence. *Neuron* **95**(2):245–258.
- He K, Zhang X, Ren S, Sun J (2015) Delving deep into rectifiers: Surpassing human-level performance on imagenet classification In *Proceedings of the IEEE international conference on computer vision*, pp. 1026–1034.
- He K, Zhang X, Ren S, Sun J (2016) Deep residual learning for image recognition In *Proceedings of the IEEE conference on computer vision and pattern recognition*, pp. 770–778.
- Heckman C, Mottram C, Quinlan K, Theiss R, Schuster J (2009) Motoneuron excitability: the importance of neuromodulatory inputs. *Clinical Neurophysiology* **120**(12):2040–2054.
- Hinton GE, Salakhutdinov RR (2006) Reducing the dimensionality of data with neural networks. *science* **313**(5786):504–507.
- Hodgkin AL, Huxley AF (1952) A quantitative description of membrane current and its application to conduction and excitation in nerve. *The Journal of physiology* **117**(4):500–544.
- Ioffe S, Szegedy C (2015) Batch normalization: Accelerating deep network training by reducing internal covariate shift. *arXiv preprint arXiv:1502.03167*.
- Kingma DP, Ba J (2014) Adam: A method for stochastic optimization. *arXiv preprint arXiv:1412.6980*.
- Klambauer G, Unterthiner T, Mayr A, Hochreiter S (2017) Self-normalizing neural networks In *Advances in Neural Information Processing Systems*, pp. 972–981.
- Korenbrodt JI (2012) Speed, sensitivity, and stability of the light response in rod and cone photoreceptors: facts and models. *Progress in retinal and eye research* **31**(5):442–466.
- LeCun Y, Bottou L, Bengio Y, Haffner P (1998a) Gradient-based learning applied to document recognition. *Proceedings of the IEEE* **86**(11):2278–2324.
- LeCun Y, Bottou L, Orr GB, Müller KR (1998b) Efficient backprop In *Neural networks: Tricks of the trade*, pp. 9–50. Springer.
- Nair V, Hinton GE (2010) Rectified linear units improve restricted boltzmann machines In *Proceedings of the 27th international conference on machine learning (ICML-10)*, pp. 807–814.
- Rosenblatt F (1958) *The perceptron: a theory of statistical separability in cognitive systems (Project Para)* Cornell Aeronautical Laboratory.
- Springenberg JT, Dosovitskiy A, Brox T, Riedmiller M (2014) Striving for simplicity: The all convolutional net. *arXiv preprint arXiv:1412.6806*.
- Szegedy C, Liu W, Jia Y, Sermanet P, Reed S, Anguelov D, Erhan D, Vanhoucke V, Rabinovich A (2015) Going deeper with convolutions In *2015 IEEE Conference on Computer Vision and Pattern Recognition (CVPR)*.